

# IMPLEMENTATION OF RAPID THERMAL PROCESSING TO ACHIEVE GREATER THAN 15% EFFICIENT SCREEN-PRINTED RIBBON SILICON SOLAR CELLS

A. Rohatgi<sup>1</sup>, V. Yelundur<sup>1</sup>, J-W. Jeong<sup>1</sup>, D.S. Kim<sup>1</sup>, A.M. Gabor<sup>2</sup>

1. University Center of Excellence for Photovoltaics Research and Education, Georgia Institute of Technology,  
777 Atlantic Dr. Atlanta, GA, U.S.A. 30332

2. Evergreen Solar, 259 Cedar Hill St. Marlboro, MA, U.S.A. 01752

## ABSTRACT

This paper summarizes our progress in fabricating record-high efficiency ribbon Si solar cells with screen-printed and photolithography defined contacts. We have developed and optimized rapid thermal processing enhanced SiN<sub>x</sub>-induced hydrogenation to achieve record-high efficiency screen-printed EFG (15.9%) and String Ribbon (15.6%) cells and a high-efficiency String Ribbon cell (17.8%) with photolithography defined contacts. A low-frequency SiN<sub>x</sub> film and a two-step RTP firing process were critical in achieving high-efficiency screen-printed cells. Step 1 provides SiN<sub>x</sub> induced hydrogenation and forms an aluminum doped back surface field. Step 2 is designed for Ag grid firing and includes rapid cooling to retain hydrogen introduced in Step 1.

## 1. INTRODUCTION

EFG and String Ribbon Si are among the most promising candidates to achieve both low-cost and high-efficiency cells because of efficient use of Si feedstock; and elimination of mechanical sawing steps, deep surface damage etching, and kerf losses. However, these materials have a high density of crystalline defects and relatively high concentrations of impurities that reduce the minority carrier lifetime in the as-grown material to typically less than 3 μs, which is not sufficient for high-efficiency cells. Therefore, effective lifetime-enhancement techniques must be implemented during cell fabrication to achieve high efficiencies. Though lamp-heated conveyor belt furnaces are preferred by the PV industry today for diffusion and metallization steps, RTP provides a promising option for low-cost and high-efficiency Si solar cells in the near future because of fast processing, accurate temperature control, and beneficial optical effects due to high-energy photons in the visible and ultra-violet range.

This paper reports on the implementation and optimization of RTP enhanced SiN<sub>x</sub>-induced hydrogenation to achieve record-high efficiency solar cells with both screen-printed and photolithography defined (PL) contacts. For screen-printed EFG and String Ribbon cells, a two-step RTP firing cycle was critical in achieving high efficiencies. Step 1 provides effective SiN<sub>x</sub>-induced hydrogenation and is designed to have a fast ramp-up rate to improve Al-BSF quality, but is not suitable for sintering the Ag contacts. Step 2, also performed in RTP, is designed for optimal Ag contact sintering and high retention of hydrogen at defects introduced in Step 1. Our previous work has shown that rapid thermal firing (RTF) improves EFG and String Ribbon cell performance by about 2% absolute over slow, belt furnace firing [1]. We

have found that rapid contact firing in RTP reduces junction shunting without degrading series resistance, resulting in a higher fill factor when compared to slow belt firing. In this work, cells benefited from optimized RTP cycles designed for PECVD SiN<sub>x</sub>-induced hydrogen passivation of bulk defects, good ohmic contacts, and the formation of an effective aluminum-doped back surface field.

## 2. EXPERIMENTAL

Solar cells with screen-printed and PL contacts were fabricated on ~300 μm thick and ~3 Ω-cm EFG and String Ribbon Si using a very simple n<sup>+</sup>-p-p<sup>+</sup> cell design. Phosphorus diffusion was performed in a conveyor belt furnace or a POCl<sub>3</sub> tube furnace to form the n<sup>+</sup>-emitter with a sheet resistance of 45-50 Ω/sq. For cells with PL contacts, the POCl<sub>3</sub> diffusion temperature was adjusted to obtain a sheet resistance of 80-90 Ω/sq. A silicon nitride (SiN<sub>x</sub>) antireflection (AR) coating was deposited on top of the n<sup>+</sup> emitter in commercial low-frequency (kHz range) and high-frequency (13.56 MHz) plasma enhanced chemical vapor deposition (PECVD) reactors. SiH<sub>4</sub>, NH<sub>3</sub>, and N<sub>2</sub> gases were used to deposit the SiN<sub>x</sub> coating with an average refractive index of 2.1 and thickness of 775 Å. A commercial Al paste (*Ferro FX-53-038*) was printed on the entire backside of all wafers and annealed in a single wafer RTP system at temperatures in the range of 600-800°C. This simultaneous anneal of Al and SiN<sub>x</sub> involves fast ramp-up and cooling rates to promote and enhance PECVD SiN<sub>x</sub>-induced hydrogen passivation of defects Si. A grid pattern was screen printed using a commercial Ag paste (*Ferro 3349*) on top of the SiN<sub>x</sub> AR coating and fired through SiN<sub>x</sub> rapidly at 700°C for 1 s in RTP to form ohmic contact to the n<sup>+</sup> emitter. Cells were isolated using a dicing saw and annealed in forming gas (10% H<sub>2</sub> in N<sub>2</sub>) at 400°C for ~10 min. Minority carrier lifetime measurements were performed at various stages of cell processing to understand and optimize defect passivation. Before minority carrier lifetime measurements, the metallization, SiN<sub>x</sub> film, and diffused layers were removed and surfaces were passivated by immersion in an I<sub>2</sub>/methanol solution. Lifetime measurements were made using the QSSPC technique at an excess carrier concentration of 10<sup>15</sup> cm<sup>-3</sup>.

## 3. RESULTS AND DISCUSSION

### 3.1 Investigation of the effect of plasma frequency on hydrogenation during deposition of PECVD SiN<sub>x</sub> films

It is well known that heat treatment of a PECVD  $\text{SiN}_x$  film is necessary to inject atomic hydrogen into the Si substrate for defect passivation. The effect of the post deposition anneal temperature on the hydrogen passivation of defects in EFG Si from both low-frequency and high-frequency  $\text{SiN}_x$  films is shown in Fig. 1. The data shows that spatially averaged lifetimes as high as 25  $\mu\text{s}$  can be attained when a high-frequency  $\text{SiN}_x$  film is annealed on EFG at 850°C. In contrast, a low-frequency  $\text{SiN}_x$  film enhances the spatially averaged lifetime to a maximum of 48  $\mu\text{s}$  when annealed at 750°C. The as-grown lifetime of the EFG samples in Fig. 1 was 1.9  $\mu\text{s}$ . The enhancement of the lifetime and hydrogenation of defects in EFG during low-frequency  $\text{SiN}_x$  film deposition and anneal is

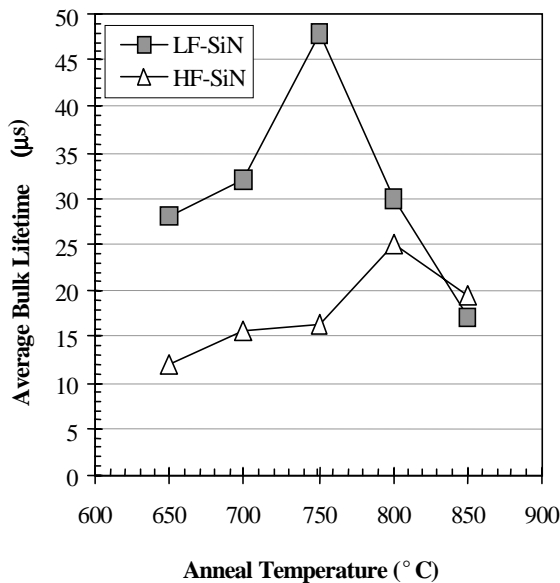


**Fig. 1** Comparison of hydrogenation from high-frequency and low-frequency  $\text{SiN}_x$  deposition and RTP anneal at various temperatures on EFG Si.

attributed to the incorporation of H during plasma deposition. During low-frequency film deposition, ions can be accelerated and implanted into the EFG substrate. However during high-frequency film deposition, reactant ions in the plasma are “frozen” with respect to the oscillation of the RF field and are not accelerated and implanted into the EFG substrate. The damage created by ion implantation near surface of the EFG substrate is believed to increase the incorporation of H. When the sample is annealed, H is released from processing-induced traps near the surface and from the nitride film and is available for defect passivation [2]. Two key observations in Fig. 1 are: a) both types of nitride films exhibit an optimum anneal temperature; and b) the optimum anneal temperature is different for the two films. The origins of the optimum hydrogenation temperature and its effect on  $V_{oc}$  are discussed in the next section.

### 3.2 Fundamental understanding of the effect of $\text{Al/SiN}_x$ anneal temperature on defect passivation and the performance of ribbon Si solar cells

The effect of the  $\text{Al/SiN}_x$  RTP anneal temperature on the average  $V_{oc}$  of screen-printed 4-cm<sup>2</sup> EFG and 49-cm<sup>2</sup> String Ribbon cells is shown in Fig. 2. For comparison, the average  $V_{oc}$  of String Ribbon cells with co-fired Al

and Ag contacts annealed at 700°C/1s in RTP is also shown (583 mV). Fig. 2 shows that two-step firing in which the hydrogenation anneal (Step 1) is performed at temperatures in the range of 600°C-700°C improves the  $V_{oc}$  of String Ribbon cells by 4-7 mV over co-fired cells. As the hydrogenation anneal (Step 1) temperature is increased to 740°C, the average  $V_{oc}$  of String Ribbon cells increases to 596 mV, a 13 mV improvement over co-

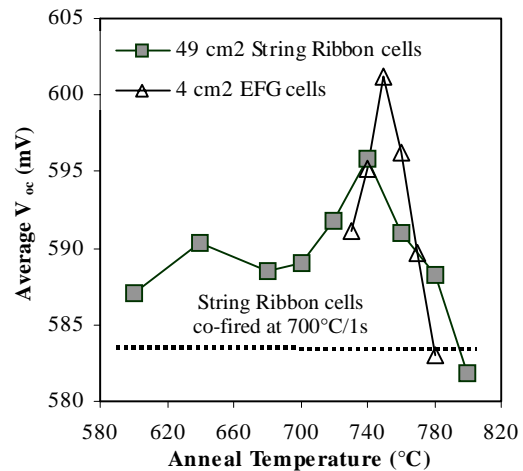


**Fig. 2** Optimization of first RTP firing step for screen-printed EFG and String Ribbon Si solar cells.

firing. As the anneal temperature is increased to 800°C, the  $V_{oc}$  decreases to 582 mV, a decrease of 1 mV when compared to co-firing. A similar dependence on the hydrogenation anneal temperature is exhibited by EFG cells, in which the average  $V_{oc}$  reaches a maximum of 601 mV at 750°C. Fig. 2 shows that the optimum hydrogenation anneal (Step 1) temperature for EFG and String Ribbon cells occurs at 750°C and 740°C respectively, and is consistent with a maximum in lifetime enhancement shown in Fig. 1 and the LBIC response shown in Fig. 3.

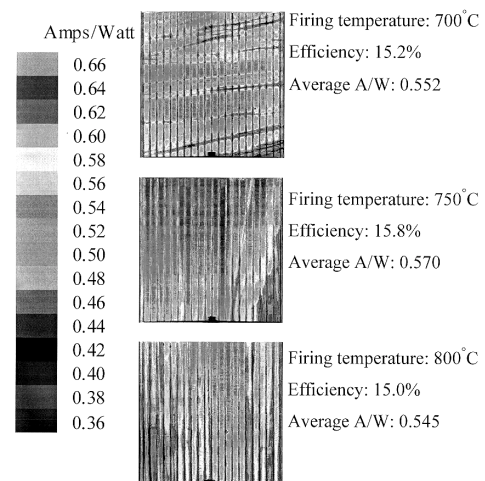


**Fig. 3** LBIC response of EFG Si cells with photolithography-defined contacts fired at 700°C, 750°C, and 800°C for 60 s in RTP (Step 1).

Figs. 1 and 2 suggest that there are competing factors in the hydrogenation process that lead to the formation of

an optimum hydrogenation temperature. Sopori et al. [2] have proposed a model for the diffusion of hydrogen in Si that includes trapping and de-trapping of hydrogen at defect sites in Si. This model is based on the formation of processing induced traps during PECVD film deposition and hydrogen trapping and de-trapping from these traps. This model along with a model that we have previously proposed [3] can be used to understand the development of an optimum hydrogenation temperature. The optimum hydrogenation temperatures observed in ribbon Si materials are the result of competition between the release of atomic hydrogen from  $\text{SiN}_x$  and/or H traps in Si and retention of hydrogen at defects in Si as illustrated in Fig. 4. In Fig. 4, hydrogenation from both low-frequency (LF- $\text{SiN}_x$ ) and high-frequency (HF- $\text{SiN}_x$ )  $\text{SiN}_x$  films is

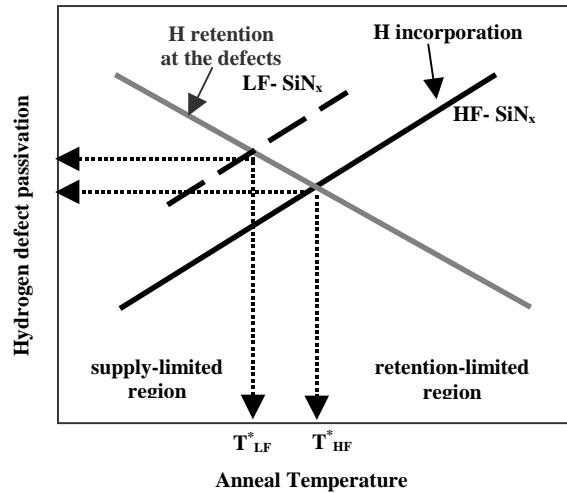


**Fig. 4** Illustration of the formation of an optimum hydrogenation anneal temperature from the competition between H incorporation and retention.

represented by two H incorporation curves. The incorporation of H from both LF- $\text{SiN}_x$  and HF- $\text{SiN}_x$  films increases with anneal temperature because more hydrogen is released from the  $\text{SiN}_x$  film. However, more H is available in the case of LF- $\text{SiN}_x$  due to the incorporation of H in Si near the surface due to the presence of a damage layer created during  $\text{SiN}_x$  deposition. At temperatures below the optimum, hydrogenation of bulk defects is limited by the low release of atomic hydrogen from the  $\text{SiN}_x$  film and/or H traps in the substrate. As the anneal temperature is increased, more hydrogen is released from the  $\text{SiN}_x$  film and/or trap sites in Si. Additionally, Al-Si alloying begins to play a role in hydrogenation. Vacancies generated by the Al alloying process enhance hydrogenation by increasing the flux of hydrogen into Si and split molecular hydrogen into atomic hydrogen. Opposing H incorporation is the retention of H at defect sites in Si. It is well known that H evolves from defect sites in Si at temperatures above  $400^\circ\text{C}$ . The retention of H at defect sites decreases as the anneal temperature increases and is represented by the gray curve in Fig. 4, and may be influenced by the cooling rate after the anneal. The optimum anneal temperatures occur at the intersection of the H retention line and H incorporation lines for LF- $\text{SiN}_x$  and HF- $\text{SiN}_x$ . At temperatures above the optimum, the retention of hydrogen at defect sites is low and hydrogenation decreases. Therefore, the optimum hydrogenation temperature represents a balance between the release of hydrogen from trap sites and the  $\text{SiN}_x$  film

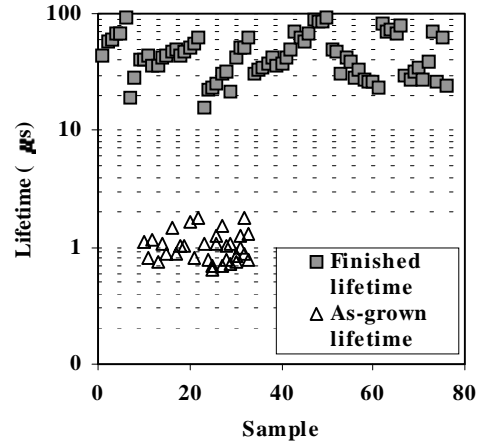


**Fig. 5** Lifetime enhancement in many String Ribbon Si samples with as-grown lifetimes below  $2 \mu\text{s}$ .

and the retention of hydrogen at electrically active defects in Si. The optimum hydrogenation temperature for LF- $\text{SiN}_x$  is lower because Si surface damage provides additional source of hydrogen and the defect passivation is strongly limited by the retention. The combination of low-frequency  $\text{SiN}_x$  induced hydrogenation and optimized RTP anneals has been very effective in raising the bulk lifetime from less than  $2 \mu\text{s}$  to well above  $20 \mu\text{s}$ . Fig. 5 shows the lifetime enhancement in many String Ribbon samples, which have an as-grown lifetime below  $2 \mu\text{s}$ . The processed lifetime was also found to be in the range of  $25\text{--}90 \mu\text{s}$  for EFG samples. We have found that  $T_{\text{LF}}^* = 740\text{--}750^\circ\text{C}$  and  $T_{\text{HF}}^* = 850^\circ\text{C}$  for hydrogenation of ribbon Si materials. Unfortunately, co-firing the Al and Ag contacts at these temperatures damages the junction and reduces the fill factor. In the next section, we implement a two-step firing scheme for screen-printed cells. The impact of rapid cooling of ribbon Si solar cells will be examined in the next section.

### 3.3 Role of two-step firing in achieving high-efficiency ribbon cells

We have found that a two-step firing scheme in RTP is vital to the fabrication of high-efficiency screen-printed ribbon Si solar cells. The first firing step is performed at  $740\text{--}750^\circ\text{C}$  for 60s and releases hydrogen from the  $\text{SiN}_x$  film and from traps near the surface of the substrate. An Al-BSF is also formed in this step. The second firing step is dedicated to Ag paste firing and is designed with rapid cooling to retain the hydrogen introduced during the first firing step. We have shown that rapid cooling, implemented after an RTP anneal, enhances the lifetime by reducing the dehydrogenation of defects [1]. To illustrate the importance of two-step firing, EFG Si cells were fabricated using three different firing schemes: a) two-step firing in a conveyor belt furnace (simultaneous firing of the PECVD  $\text{SiN}_x$  and the screen-printed Al at  $850^\circ\text{C}$  for 2 min followed by  $730^\circ\text{C}/10\text{s}$  firing for the screen-printed Ag contacts), b) co-firing at  $730^\circ\text{C}$  in a conveyor belt furnace, and c) co-firing at  $700^\circ\text{C}$  in the RTP system. Scheme d) corresponds to two-step RTP firing ( $760^\circ\text{C}/60\text{s} + 700^\circ\text{C}/1\text{s}$ ). Bulk lifetimes were measured before and after each process scheme by quasi-steady-state photoconductance (QSSPC) method to assess the process-induced lifetime change.

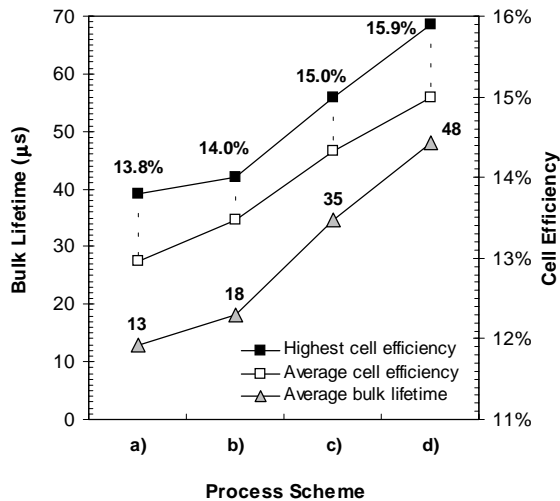


**Fig. 6** The bulk lifetime and cell efficiency of screen-printed EFG Si cells after four different firing schemes.

Fig. 6 shows bulk lifetime and cell efficiency after the four different process schemes. Scheme d) involves the two-step RTP firing, and produced the best results. The as-grown lifetime of the EFG Si samples was only  $\sim 2$   $\mu\text{s}$ , which improved to a) 13  $\mu\text{s}$  after the two-step belt furnace firing process, b) 18  $\mu\text{s}$  after the co-firing process in the belt furnace, c) 35  $\mu\text{s}$  after the co-firing in the RTP, and d) 48  $\mu\text{s}$  after the two-step RTP firing process. Fig. 6 also shows that a) the two-step belt furnace firing process resulted in an average efficiency of 13.0% with a maximum of 13.8%, b) the belt furnace co-firing gave an average efficiency of 13.5% with a maximum of 14.0%, c) the RTP co-firing produced an average efficiency of 14.3% with a maximum of 15.0%, and d) the two-step RTP firing process resulted in an average efficiency of 15.0% with a maximum of 15.9% (confirmed by NREL). Fig. 6 shows that belt-fired cells, where cooling was much slower than RTP, have lower bulk lifetime and efficiency. In addition, the fast ramp-up rate in RTP improves the uniformity and quality of Al-BSF further enhancing cell performance. Optimized screen-printed Ag contact firing

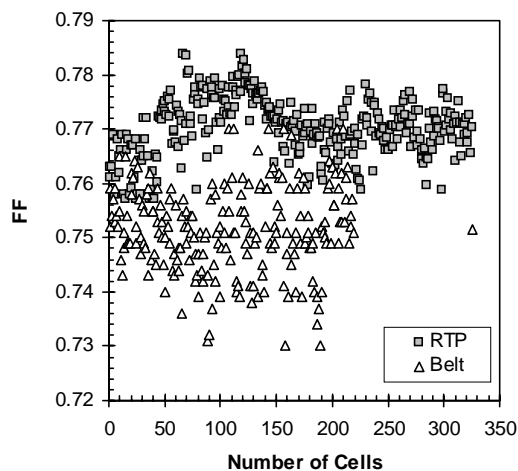


**Fig. 7** Comparison of FF distribution of a large number of screen-printed EFG Si cells with Ag contact firing in RTP ( $700^\circ\text{C}/1\text{s}$ ) and belt furnace ( $740^\circ\text{C}/45\text{s}$ ).

at  $700^\circ\text{C}$  (Step 2) also contributed to high efficiency because the very short firing time with rapid cooling rate helped in retaining hydrogen at defects that was

**Table I.** Cell parameters for high-efficiency ribbon cells with low-frequency  $\text{SiN}_x$  hydrogenation and RTP firing.

Material	Front contact	Voc (mV)	Jsc ( $\text{mA}/\text{cm}^2$ )	FF	Eff. (%)
String Ribbon	Vacuum evap.	622	36.4	0.785	17.8
String Ribbon	Screen-printed	606	33.8	0.762	15.6
EFG	Screen-printed	615	33.7	0.769	15.9

incorporated in Step 1. We have found that rapid thermal firing of screen-printed contacts improves the FF response when compared to belt furnace firing (Fig. 4).

RTP firing has been applied to screen-printed String Ribbon solar cells with  $\text{SiN}_x$  AR coatings to achieve noteworthy efficiencies as high as 15.6% (confirmed by NREL) and 17.8% (confirmed by NREL) in cells with PL defined contacts and a two-layer AR coating ( $\text{SiN}_x/\text{MgF}_2$ ). The parameters of these high-efficiency,  $4\text{-cm}^2$  ribbon Si solar cells are shown in Table I.

#### 4. CONCLUSION

We have developed and optimized RTP enhanced  $\text{SiN}_x$  induced hydrogenation to achieve record-high efficiency ribbon Si solar cells with screen-printed and photolithography defined contacts. A two-step RTP firing cycle was critical in achieving high efficiency screen-printed EFG (15.9%) and String Ribbon (15.6%) cells. Step 1 provides  $\text{SiN}_x$  induced hydrogenation and forms an Al-BSF. Step 2 is designed for optimal Ag grid sintering and implements rapid cooling to retain hydrogen introduced in Step 1. A  $\text{SiN}_x$  film deposited by PECVD at a lower frequency was found to be more effective in hydrogen passivation of defects.

#### 5. REFERENCES

- [1] V. Yelundur, A. Rohatgi, J-W. Jeong, and J.I. Hanoka, "Improved String Ribbon Si solar cell performance by rapid thermal firing of screen-printed contacts", *IEEE Trans. Elec. Dev.* **49**, 1405 (2002).
- [2] B. Sopori, Y. Zhang, R. Reedy, K. Jones, N.M. Ravindra, S. Rangan, S. Ashok, "Trapping and detrapping of H in Si: Impact on diffusion properties and solar cell processing", *Proceedings of the 3<sup>rd</sup> Symposium on Defect and Impurity Engineered Semiconductors and Devices*, (MRS, San Francisco, CA, 2002) p. 125.
- [3] V. Yelundur, A. Rohatgi, A. Ebong, A.M. Gabor, J. Hanoka, R.L. Wallace, "Al-enhanced PECVD  $\text{SiN}_x$  induced hydrogen passivation in String Ribbon silicon", *J. Electr. Mats.*, **30**, 526 (2001).